Supplement of

Traceable calibration of in-situ aerosol absorption instruments with monodisperse nigrosin

Drinovec et al.

Correspondence to: Luka Drinovec (luka.drinovec@ung.si)

S1. Measurement time series

During experiment "2024_03_05 Monodisperse cpma" nigrosin particles were selected using a CPMA. Measurements of aerosol absorption, number of particles and current were measured using a PTAAM, a CPC and a FCAE correspondingly (Fig. S1).

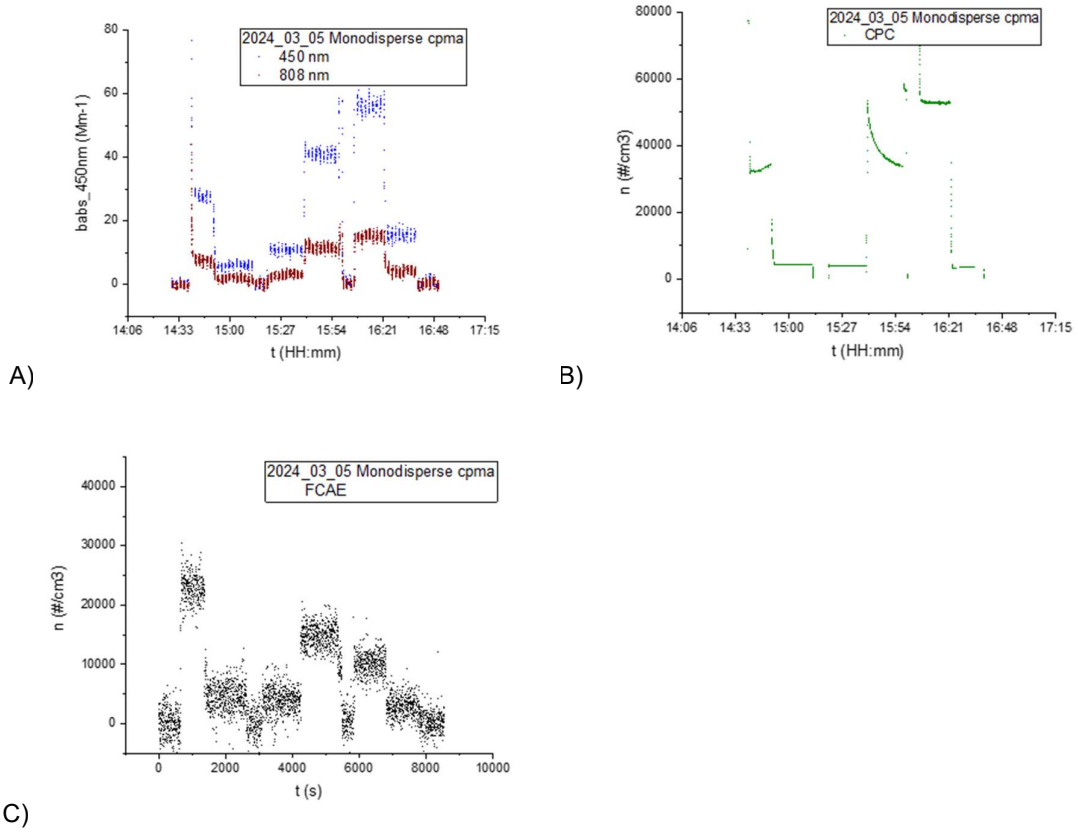

Figure S1. Time series of PTAAM (A), CPC (B) and FCAE (C) measurements for experiment "2024_03_05 Monodisperse cpma" with native 1 s time resolution.

S2. Effective density of polystyrene beads

Polystyrene beads were nebulized and sequentially analyzed with an SMPS and CPMA-CPC. Particle size/mass was determined by fitting a log-normal curve. The measured density differs from the nominal value by 0.8% (Table S1). Effective density of ammonium sulfate increases with particle mass towards the reference value of 1.77 g cm^{-3} (Haynes et al., 2017) (Fig S2).

Table S1. Reported and measured density of polystyrene beads.

	Diameter (nm)	Mass (fg)	Density (g/cm3)
Reported	95 +/- 4		1.05
Measured	94.988 +/- 0.05	0.5676 +/- 0.0005	1.042 +/- 0.002

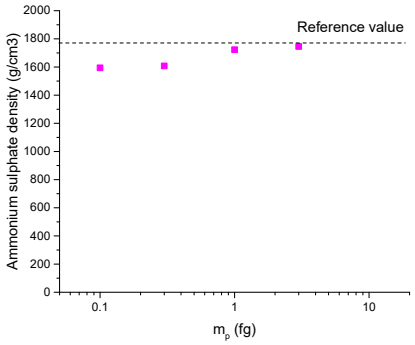

Figure S2. Effective density of nebulized ammonium sulfate particles.

S3. Mass absorption cross-section of nigrosin at 450 and 808 nm

The theoretical mass absorption cross-section of nigrosin was calculated using Mie theory based on a particle density of 1.6 g/cm3 for refractive index values of 1.58 + i0.167 at 450 nm and 1.78 + i0.119 at 808 nm.

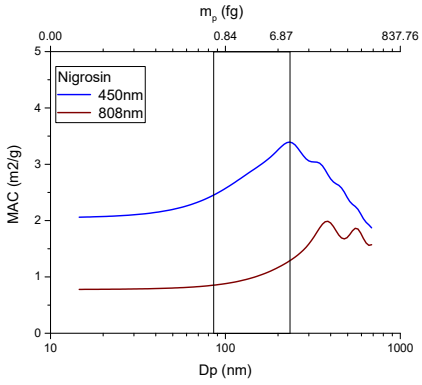

Figure S3. Mie calculated mass absorption cross-section for nigrosin particles of different sizes assuming a density of 1.6 g $^{cm-3}$.

S4. Measurement of multiply-charged particles in DMA-selected nigrosin

CPMA-CPC were installed after a DMA to measure number vs. mass particle distribution. Data were fitted with multiple log-normal peak functions.

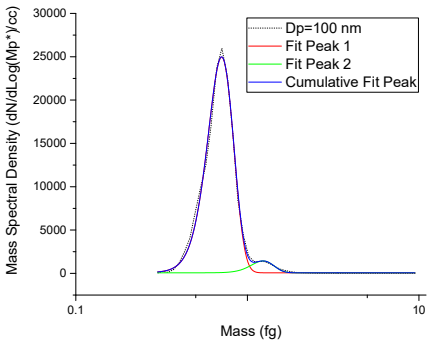

A)

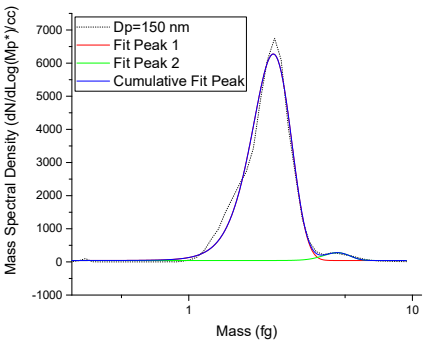

B)

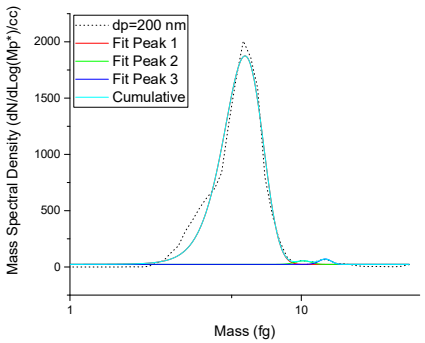

C)

Figure S4. Number mass distribution of monodisperse nigrosin with mobility diameters of 100 nm (A), 150 nm (B) and 200 nm (C).

S5. SEM image of fused nigrosin particles

Nigrosin particles were collected on Nucleopore filters and analyzed using a scanning electron microscope FEI HeliosNanolab 650 (Thermo Fisher Scientific, USA) operated at 1 kV accelerating voltage. The samples were mounted on SEM holders with a carbon tape and coated with a few nanometers of carbon to prevent charging effects.

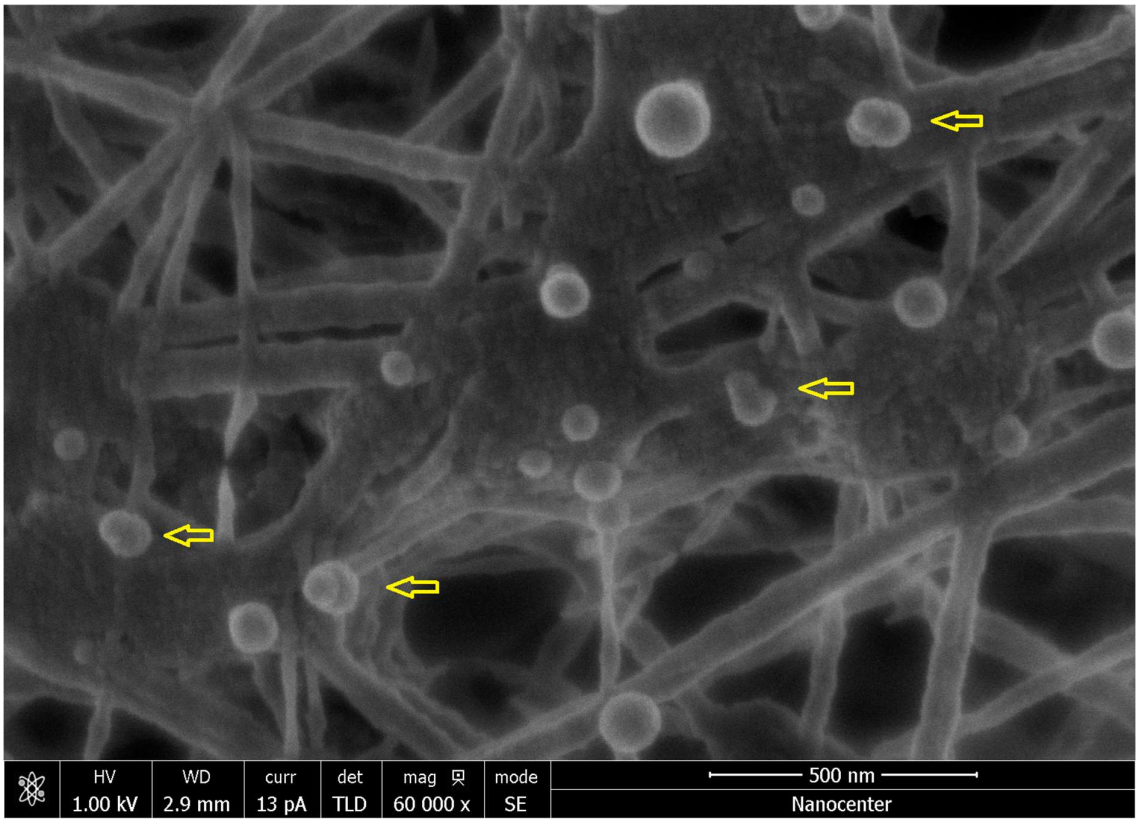

Figure S5. Scanning electron micrograph of nigrosin particles. Arrows designate fused, non-completely-spherical particles.

S6. Measured and calculated absorption of monodisperse nigrosin at 450 and 808 nm

The 450 nm channel of PTAAM was calibrated using NO_2, while the 808 nm channel was calibrated by transferring calibration from the 450 nm channel using the Mie-calculated absorption ratio $b_{abs\_808nm}/b_{abs\_450nm}$ for polydisperse nigrosin as described in Drinovec et al., 2022. PTAAM measurements are compared with Mie calculated absorption coefficient based on mobility diameter and mass equivalent diameter (Fig. S6 & Table S2).

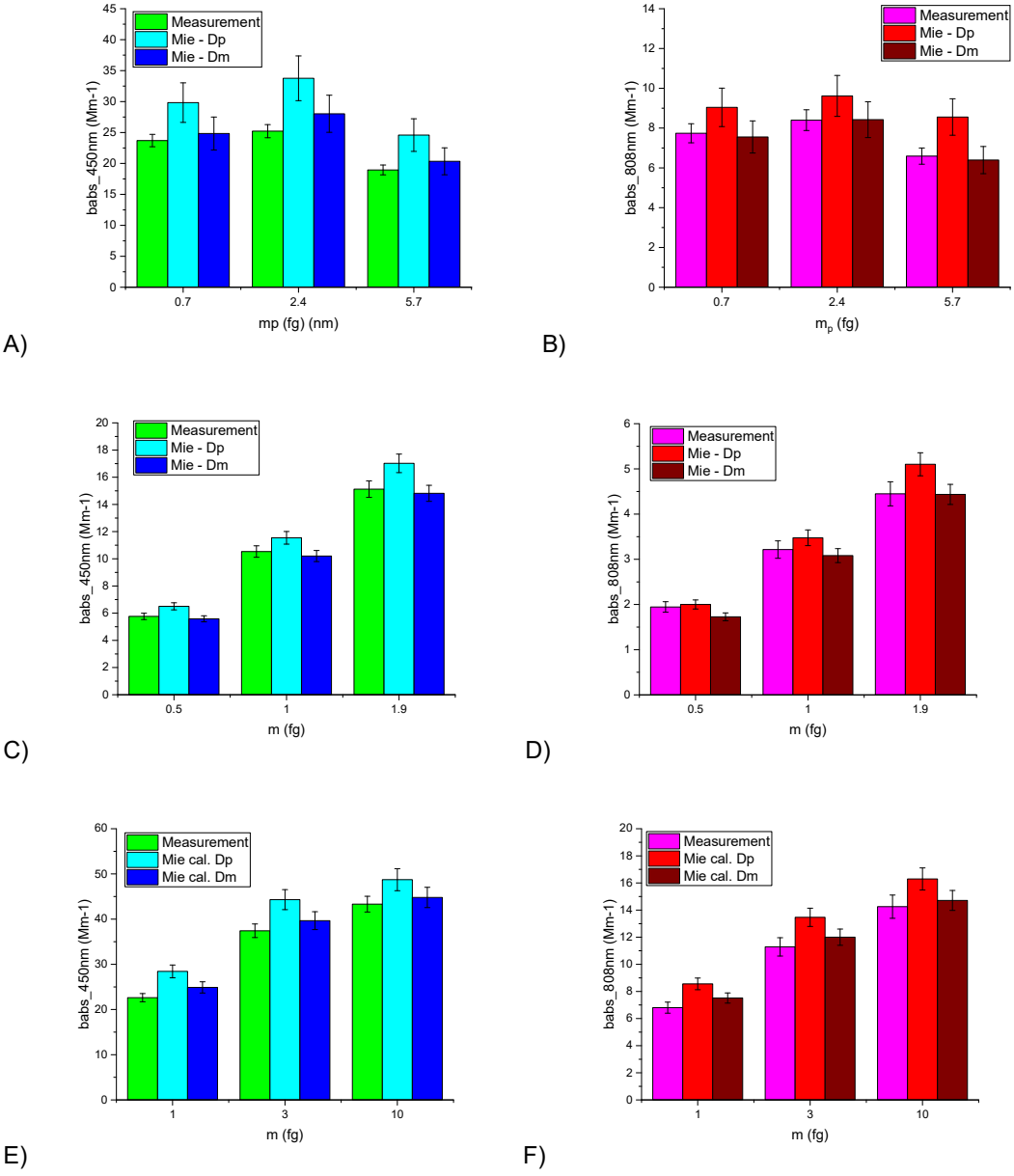

Figure S6. Measured and calculated absorption coefficient of monodisperse nigrosin at 450 nm (left: A, C, E) and 808 nm (right: B, D, F). Nigrosin was size-selected using a DMA (A & B), a CPMA (C & D) and a tandem of CPMA and DMA (E & F). Error bars represent measurement uncertainty.

Table S2. Measured and calculated absorption coefficient of monodisperse nigrosin at 450 nm and 808 nm. Nigrosin was size-selected using a DMA, a CPMA and a tandem of CPMA and DMA. Error represents measurement uncertainty.

Selection method	mp (fg)	Dp (nm)	babs_450nm (Mm-1)			babs_808nm (Mm-1)		
			PTAAM	Mie_Dp	Mie_Dm	PTAAM	Mie_Dp	Mie_Dm
DMA	0.7	100	23.7 ± 1	29.8 ± 3.2	24.8 ± 2.7	7.74 ± 0.5	9.0 ± 1.0	7.6 ± 0.8
DMA	2.4	150	25.2 ± 1.1	33.8 ± 3.6	28.0 ± 3.0	8.4 ± 0.5	9.6 ± 1.0	8.4 ± 0.9
DMA	5.7	200	19.0 ± 0.8	24.6 ± 2.6	20.3 ± 2.2	6.6 ± 0.4	8.6 ± 0.9	6.4 ± 0.7
CPMA	0.5	88.2	5.8 ± 0.2	6.5 ± 0.4	5.6 ± 0.3	1.95 ± 0.1	2.00 ± 0.1	1.73 ± 0.1
CPMA	1.0	110.1	10.5 ± 0.4	11.5 ± 0.7	10.2 ± 0.6	3.2 ± 0.2	3.5 ± 0.2	3.1 ± 0.2
CPMA	1.9	137.0	15.1 ± 0.6	17.0 ± 1	14.8 ± 0.9	4.4 ± 0.3	5.1 ± 0.3	4.4 ± 0.2
Tandem	1.0	110.4	22.8 ± 0.9	28.4 ± 1.4	24.9 ± 1.2	6.8 ± 0.4	8.6 ± 0.4	7.5 ± 0.4
Tandem	3.0	158.2	37.9 ± 1.5	44.3 ± 2.2	39.7 ± 2.0	11.3 ± 0.7	13.5 ± 0.7	12.0 ± 0.6
Tandem	10.0	235.0	43.7 ± 1.7	48.7 ± 2.4	44.8 ± 2.2	14.3 ± 0.9	16.3 ± 0.8	14.7 ± 0.7

S7. Measurement of NO_2 and particle losses in PTAAM

NO_2 loses between the instrument inlet and the measurement chamber were measured by running a known concentration of NO_2 sample through the instrument and being measured with CAPS NO_2 monitor. Sample flow through the PTAAM was kept at 0.45 L min^{-1} by adding a fixed amount of NO_2 free air before entering the CAPS. NO_2 loss for sub 1 µmol mol^{-1}sample was calculated by comparing the measured NO_2 concentration running through the PTAAM with the bypass configuration.

Particle losses were determined for monodisperse and polydisperse nigrosin particle distributions. Nigrosin particles were generated using the solution with 0.1 g L^{-1} nigrosin. For monodisperse measurements the aerosol was routed through the neutralizer and the CPMA to the PTAAM. Sample was directed out of the sample cell and fixed amount of particle free sample was added before the CPC, keeping the sample flow through the instrument stable at 0.45 L min^{-1}. Measured number concentration was compared to the setup without the PTAAM. For polydisperse experiment the neutralized nigrosin particles passed the PTAAM before adding particle free air and being measured using the SMPS. The size dependent particle losses are shown in Table S3. Particle losses for single charged 100 nm particles are approx. 5%. Particle losses for mineral dust particles (Table S4) were measured in a similar manner using optical particle sizer Grimm 11-D (Durag Group, Germany).

Table S3. Measured nigrosin particle losses using monodisperse particles selected using CPMA or polydisperse particles analysed using SMPS after passing the inlet part of the PTAAM.

D_p (nm)	Loss_monodisperse	Loss_polydisperse	m_p (fg)
200	2.1%	2.9%	6.69
100	4.3%	5.6%	0.83
50	10.6%	12.5%	0.105
25	24.4%	26%	0.013
12.9	47.0%	47%	0.0018

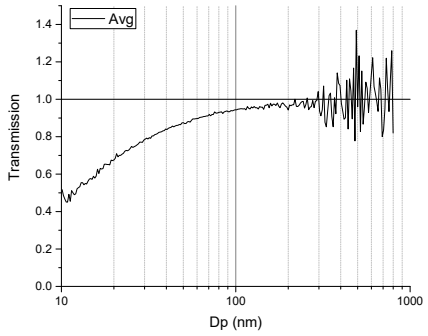

Figure S7. Penetration efficiency in PTAAM for single-charged nigrosin particles.

Table S4. Particle loss in PTAAM for different fractions of mineral dust particles

Particle size fraction	Particle loss
PM10 [ug/m3]	10.0%
PM4 [ug/m3]	9.4%
PM2.5 [ug/m3]	8.1%
PM1 [ug/m3]	3.8%

References

Drinovec, L., Jagodič, U., Pirker, L., Škarabot, M., Kurtjak, M., Vidović, K., Ferrero, L., Visser, B., Röhrbein, J., Weingartner, E., Kalbermatter, D. M., Vasilatou, K., Bühlmann, T., Pascale, C., Müller, T., Wiedensohler, A., and Močnik, G.: A dual-wavelength photothermal aerosol absorption monitor: design, calibration and performance, Atmos. Meas. Tech., 15, 3805–3825, https://doi.org/10.5194/amt-15-3805-2022, 2022.

Haynes, W.M., Lide, D.R. and Bruno, T.J. (Eds.): CRC Handbook of Chemistry and Physics, 97th Edition, CRC Press, 2017.